

1 The Morphological Diversification of Siphonophore Ten-

2 tilla

3 Alejandro Damian-Serrano^{1,‡}, Steven H.D. Haddock², Casey W. Dunn¹

4 ¹ Yale University, Department of Ecology and Evolutionary Biology, 165 Prospect St.,
5 New Haven, CT 06520, USA

6 ² Monterey Bay Aquarium Research Institute, 7700 Sandholdt Rd., Moss Landing, CA
7 95039, USA

8 ‡ Corresponding author: Alejandro Damian-Serrano, email: alejandro.damianserrano@
9 yale.edu

10 Abstract

11 Siphonophore tentilla (tentacle side branches) are unique biological structures for prey capture,
12 composed of a complex arrangement of cnidocytes (stinging cells) bearing different types of
13 nematocysts (stinging capsules) and auxiliary structures. Tentilla present an extreme mor-
14 phological diversity of form and function across species. While associations between tentilla
15 form and diet have been reported, the evolutionary history giving rise to this morphological
16 diversity is largely unexplored. Here we explore the evolutionary gains and losses of novel
17 tentilla substructures on the most recent siphonophore phylogeny. Tentilla have a precisely co-
18 ordinated high-speed strike mechanism of synchronous unwinding and nematocysts discharge.
19 Here we characterize the kinematic diversity of this prey capture reaction using high-speed
20 video and find relationships with morphological characters. Since tentillum discharge occurs
21 in synchrony across a broad morphological diversity, we evaluate how phenotypic integration is
22 maintaining character correlations across evolutionary time. Moreover, we analyze the dimen-
23 sionality of the tentillum morphospace, identify instances of heterochrony and morphological
24 convergence, and generate hypotheses on the diets of understudied siphonophore species. Our
25 findings indicate that siphonophore tentilla are phenotypically integrated structures with

²⁶ a complex evolutionary history leading to a phylogenetically structured diversity of forms
²⁷ which are predictive of kinematic performance and feeding habits.

²⁸ **Keywords**

²⁹ Siphonophore, tentilla, nematocysts, character evolution

³⁰ **Introduction**

³¹ Siphonophores have fascinated zoologists for centuries for their extremely subspecialized
³² colonial organization and integration. However, far less attention has been devoted to their
³³ unique tentacular structures: the tentilla. Like many cnidarians, siphonophore tentacles bear
³⁴ side branches (tentilla) with nematocysts. But unlike other cnidarians, most siphonophore
³⁵ tentilla are dynamic structures that react to prey encounters by shooting the nematocyst
³⁶ battery to slap around the prey. This maximizes the surface area of contact between the
³⁷ nematocysts and the prey they fire upon. Siphonophore tentilla present an exuberant diversity
³⁸ of morphologies, sizes, and nematocyst complements (Figure 1).

³⁹ In (1), we collected the most extensive morphological dataset on siphonophore tentilla and
⁴⁰ nematocysts using state-of-the-art microscopy techniques, and expanded the taxon sampling
⁴¹ of the phylogeny to disentangle the evolutionary history. The analyses we carried out led to
⁴² novel insights into the evolution of predatory specialization. However, this work left behind
⁴³ many fascinating discoveries on the evolutionary history of tentilla morphology, including
⁴⁴ nematocyst novelties, phenotypic integration, convergent evolution, paedomorphosis, and
⁴⁵ predictions on diet using morphology. Here, we present these findings and shed light on the
⁴⁶ natural history of siphonophores.

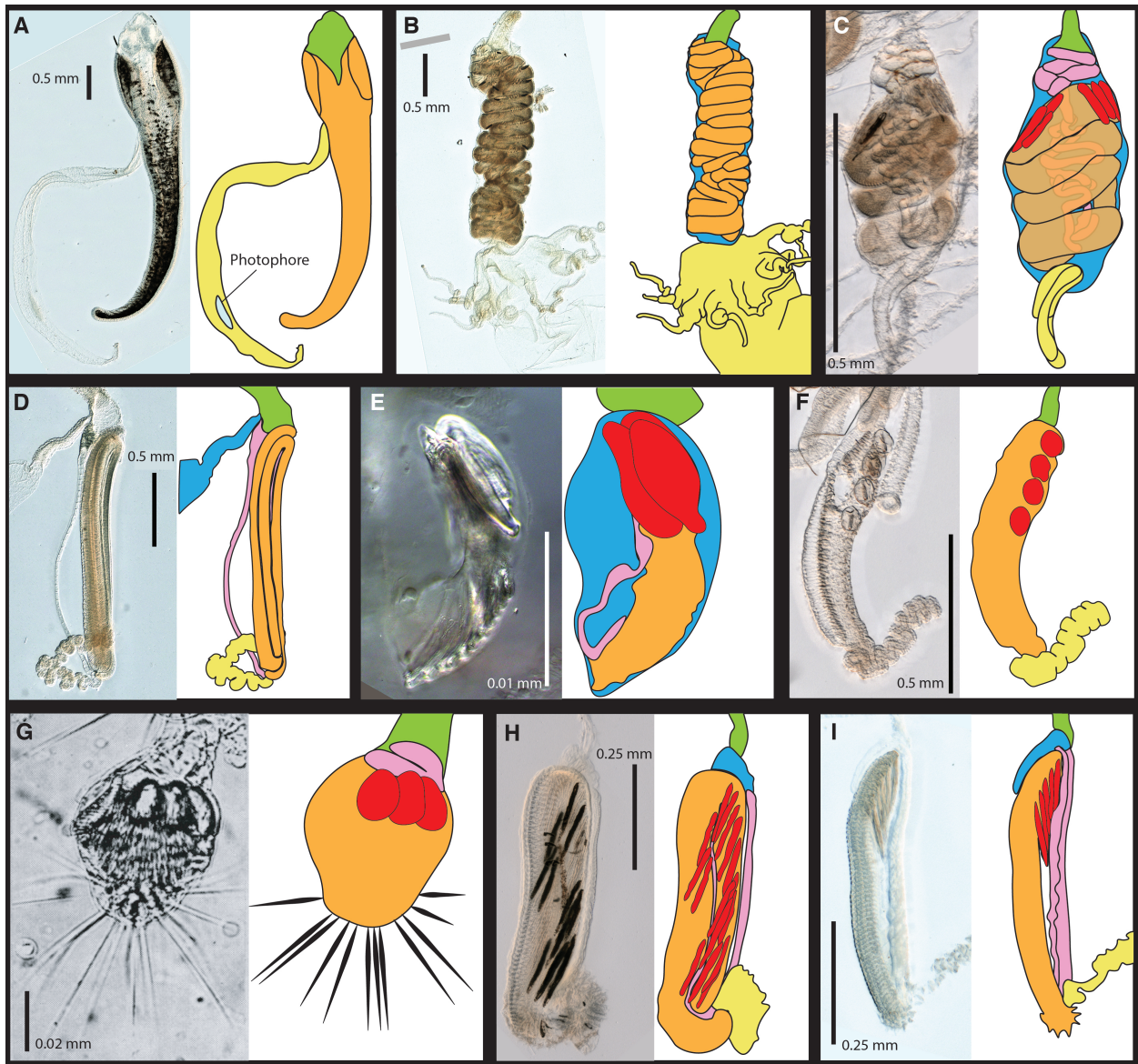
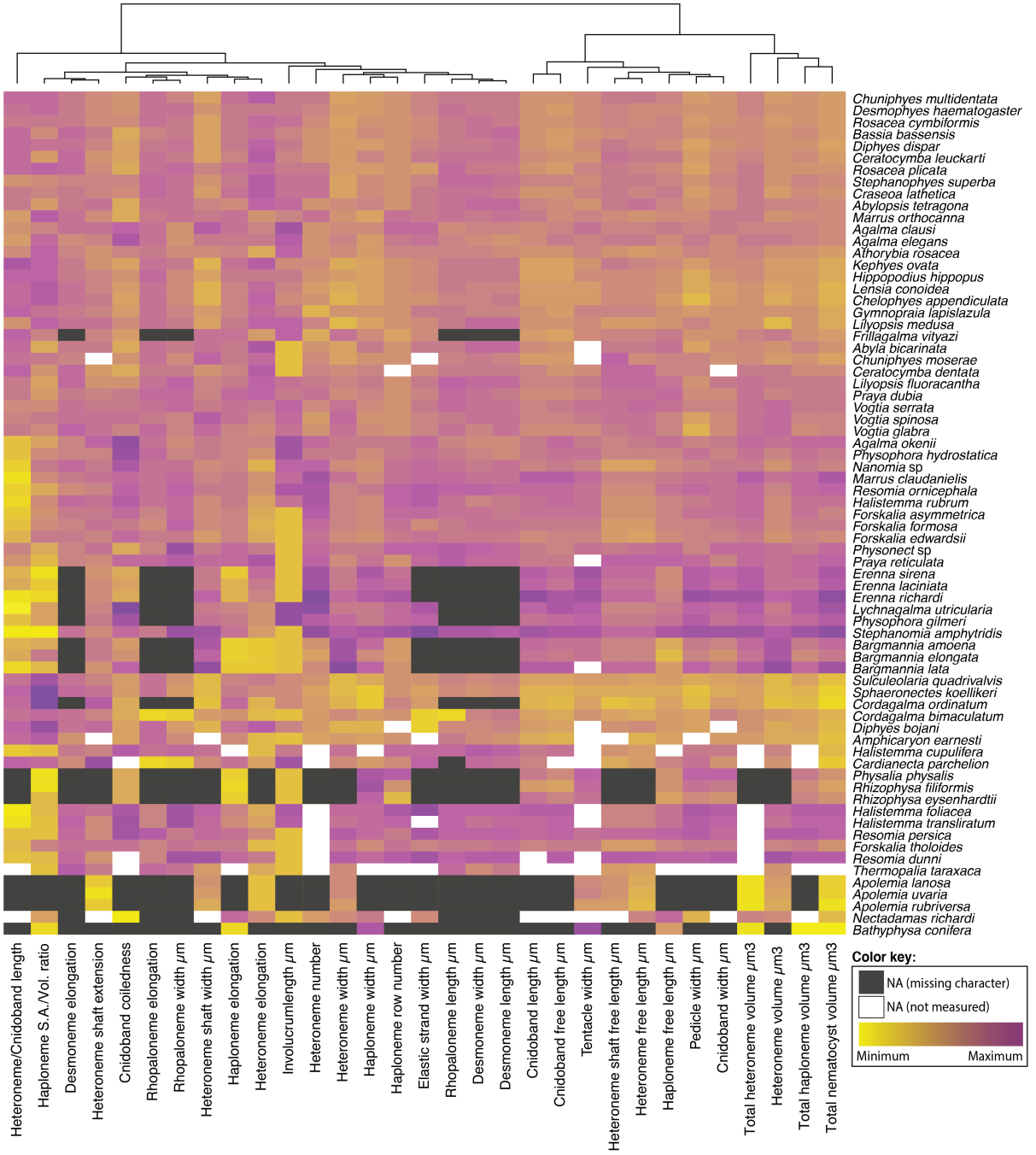


Figure 1: Tentillum diversity. The illustrations delineate the pedicle (green), involucrum (blue), cnidoband (orange), elastic strands (pink), terminal structures (yellow). Heteroneme nematocysts (stenoteles in C,E,F,G and mastigophores in H,I) are depicted in red for some species. A - *Erenna laciniata*, 10x. B - *Lychnagalma utricularia*, 10x. C - *Agalma elegans*, 10x. D - *Resomia ornicephala*, 10x. E - *Frillagalma vityazi*, 20x. F - *Bargmannia amoena*, 10x. G - *Cordagalma* sp., reproduced from Carré 1968. H - *Lilyopsis fluoracantha*, 20x. I - *Abylopsis tetragona*, 20x.

47 **Methods**

48 We explore the evolutionary history and diversification of tentilla morphologies using phyloge-
49 netic comparative methods on the morphological dataset and phylogeny published in (1). We
50 fitted different models generating the observed data distribution given the phylogeny for each
51 continuous character using the function `fitContinuous` in the R package *geiger* (2). These
52 models include a non-phylogenetic white-noise model (WN), a neutral divergence Brownian
53 Motion model (BM), an early-burst decreasing rate model (EB), and an Ornstein-Uhlenbeck
54 model with stabilizing selection around a fitted optimum trait value. We then ranked the
55 models in order of increasing parametric complexity (WN, BM, EB, OU), and compared
56 the corrected Akaike Information Criterion (AICc) support scores (3) to the lowest (best)
57 score, using a cutoff of 2 units to determine significantly better support. When the best
58 fitting model was not significantly better than a less complex alternative, we selected the
59 least complex model (SM13). We calculated model adequacy scores using the R package
60 *arbutus* (4) (SM14). We calculated phylogenetic signals in each of the measured characters
61 using Blomberg's K (5) (SM13).

62 In order to explore the correlational structure among continuous characters and among
63 their evolutionary histories, we used principal component analysis (PCA) and phylogenetic
64 PCA (6). Since the character dataset contains many gaps due to missing characters and
65 inapplicable states, we carried out these analyses on a subset of species and characters that
66 allowed for the most complete dataset. This was done by removing the terminal filament
67 characters (which are only shared by a small subset of species), and then removing species
68 which had inapplicable states for the remaining characters. In addition, we obtained the
69 correlations between the phylogenetic independent contrasts (7) using the package *rphylip*
70 (8).



71 **Results**

72 *Evolutionary history of tentillum morphology* – (1) produced the most speciose siphonophore
73 molecular phylogeny to date, while incorporating the most recent findings in siphonophore
74 deep node relationships. This phylogeny revealed for the first time that the genus *Erenna* is the
75 sister to *Stephanomia amphytridis*. *Erenna* and *Stephanomia* bear the largest tentilla among all
76 siphonophores, thus their monophyly indicates that there was a single evolutionary transition
77 to giant tentilla. Siphonophore tentilla range in size from ~30 µm in some *Cordagalma*
78 specimens to 2-4 cm in *Erenna* species, and up to 8 cm in *Stephanomia amphytridis* (9).
79 Most siphonophore tentilla measure between 175 and 1007 µm (1st and 3rd quartiles), with a
80 median of 373 µm. The extreme gain of tentillum size in this newly found clade may have
81 important implications for access to large prey size classes.

82 Siphonophore tentilla are defined as lateral, monostichous evaginations of the tentacle
83 gastrovascular lumen with epidermal nematocysts (10). The buttons on *Physalia* tentacles
84 were not traditionally regarded as tentilla, but (11) and our observations (12), confirm that
85 the buttons contain evaginations of the gastrovascular lumen, thus satisfying all the criteria
86 for the definition. In this light, and given that most Cystonectae bear conspicuous tentilla,
87 we conclude (in agreement with (12)) that tentilla are likely ancestral to all siphonophores,
88 and secondarily lost in *Apolemia* and *Bathyphysa conifera*.

89 In order to gain a broad perspective on the evolutionary history of tentilla, we reconstructed
90 the phylogenetic positions of the main categorical character shifts using stochastic character
91 mapping (SM22-30) and summarized in 3. Some of these characters include the gain and loss
92 of nematocyst types. Based on external information, we assume that haploneme nematocysts
93 are ancestrally present in siphonophore tentacles since they are present in the tentacles of
94 many other hydrozoans. Haplonemes first diverged into spherical isorhizas of 2 size classes in
95 Cystonectae, and elongated anisorhizas of one size class in Codonophora. Haplonemes were
96 likely lost in the tentacles of *Apolemia* but retained as spherical isorhizas in other *Apolemia*
97 tissues (13). Similarly, while heteronemes exist in other tissues of cystonects, they appear

98 in the tentacles of codonophorans exclusively, as birhopaloids in *Apolemia*, stenoteles in
99 eucladophoran physonects, and microbasic mastigophores in calycophorans.

100 The clades defined in (1) are characterized by unique evolutionary innovations in their
101 tentilla. The clade Eucladophora (containing Pyrostephidae, Euphysonectae, and Caly-
102 cophorae) encompasses all of the extant Siphonophore species (178 of 186) except Cystonects
103 and *Apolemia*. Innovations that arose along the stem of this group include spatially seg-
104 regated heteroneme and haploneme nematocysts, terminal filaments, and elastic strands
105 (Fig. 3). Pyrostephids evolved a unique bifurcation of the axial gastrovascular canal of
106 the tentillum known as the “saccus” (10). The stem to the clade Tendiculophora (clade
107 containing Euphysonectae and Calycophorae) subsequently acquired further novelties such
108 as the desmoneme and rhopaloneme (acrophore subtype ancestral) nematocysts on the
109 terminal filament (Fig. 3), which bears no other nematocyst type. These are arranged in
110 sets of 2 parallel rhopalonemes for each single desmoneme (14, 15). The involucrum is an
111 expansion of the epidermal layer that can cover part or all of the cnidoband (Fig. 1). This
112 structure, together with differentiated larval tentilla, appeared in the stem branch to Clade
113 A physonects. Calycophorans evolved novelties such as larger desmonemes at the distal
114 end of the cnidoband, pleated pedicles with a “hood” (here considered homologous to the
115 involucrum) at the proximal end of the tentillum, anacrophore rhopalonemes, and microbasic
116 mastigophore-type heteronemes. While calycophorans have diversified into most of the extant
117 described siphonophore species (108 of 186), their tentilla have not undergone any major
118 categorical gains or losses since their most recent common ancestor. Nonetheless, they have
119 evolved a wide variation in nematocyst and cnidoband sizes.

120 *Evolution of tentillum and nematocyst characters* – One-third of the characters measured
121 in (1) support a non-phylogenetic generative model, indicating they are not phylogenetically
122 conserved (SM7). Most (74%) characters present a significant phylogenetic signal, yet only
123 total nematocyst volume, haploneme length, and heteroneme-to-cnidoband length ratio had
124 a phylogenetic signal with K larger than 1. Total nematocyst volume and cnidoband-to-

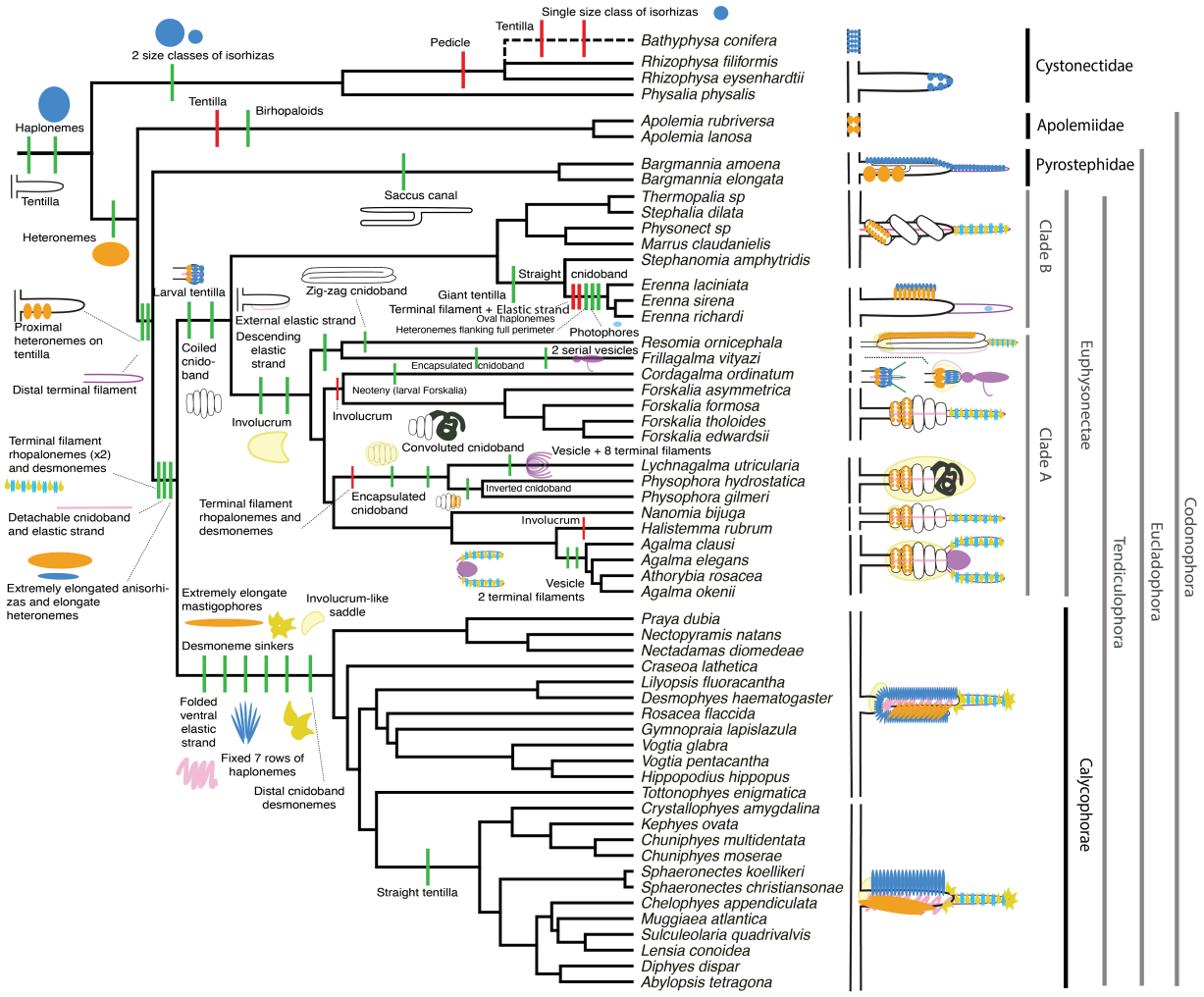
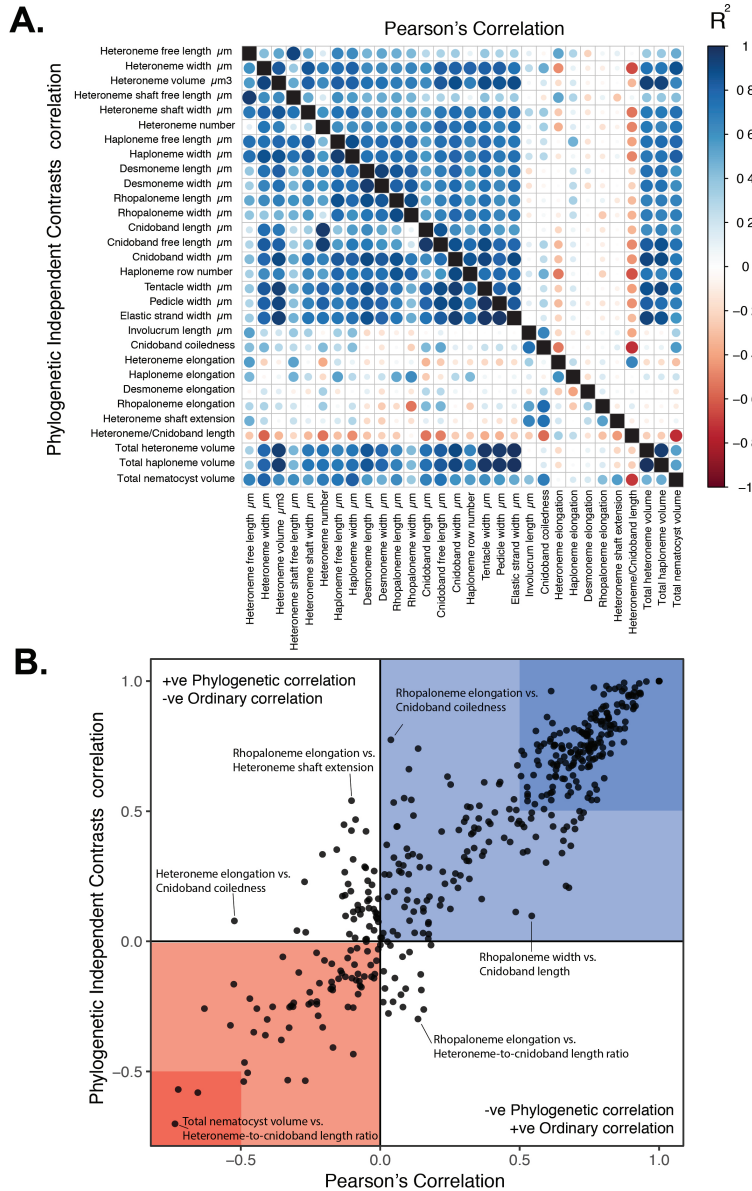


Figure 3: Siphonophore cladogram with the main categorical character gains (green) and losses (red) mapped. Some branch lengths were modified from the Bayesian chronogram to improve readability. The main visually distinguishable tentillum types are sketched next to the species that bear them, showing the location and arrangement of the main characters. In large, complex-shaped euphysonect tentilla, haplonemes were omitted for simplification. The rhizophysid *Bathyphysa conifera* branch was appended manually as a polytomy (dashed line).

125 heteroneme length ratio showed strongly conserved phylogenetic signals. The majority (67%)
 126 of characters support BM models, indicating a history of neutral constant divergence. No
 127 relationship between phylogenetic signal and BM model support was found. Haploneme
 128 nematocyst length is the only character with support for an EB model of decreasing rate
 129 of evolution with time. No character had support for a single-optimum OU model (when
 130 uninformed by feeding guild regime priors).



131

Evolution of nematocyst shape

132 – The greatest evolutionary change in haploneme nematocyst shape occurred in a single shift
 133 towards elongation in the stem of Tendiculophora, which contains the majority of described

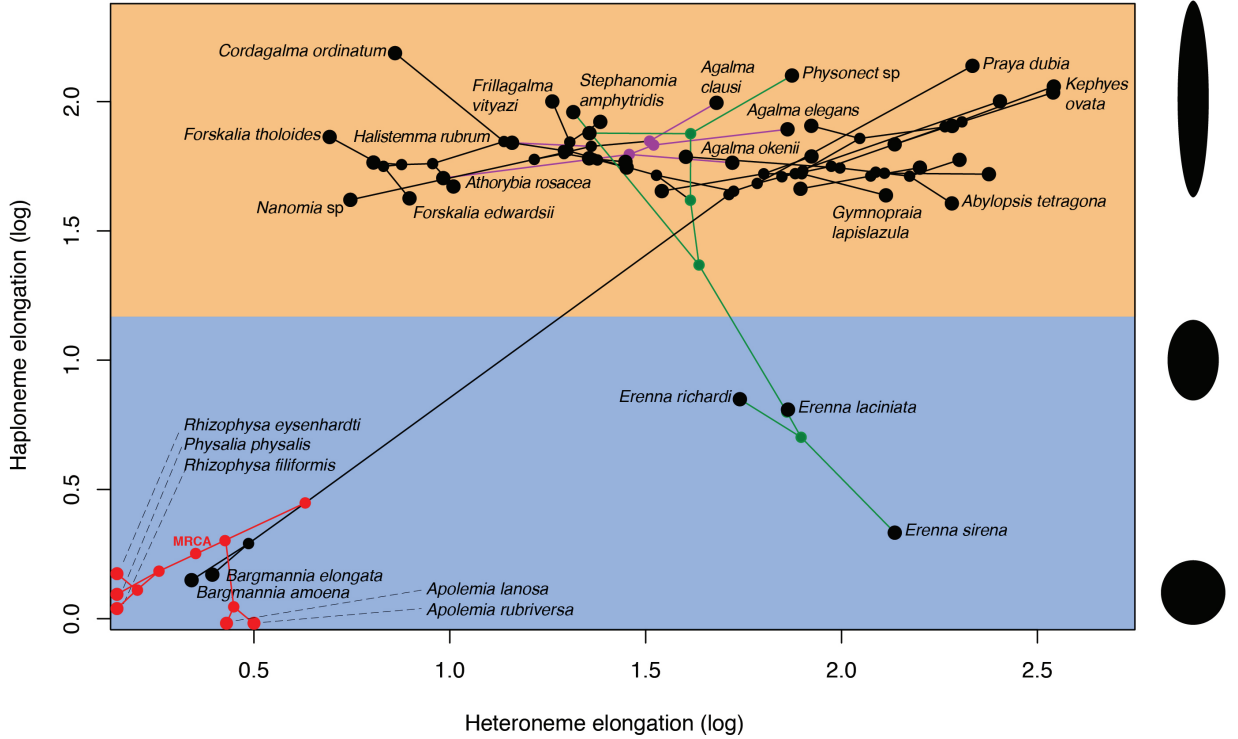


Figure 4: Phylomorphospace showing haploneme and heteroneme elongation (log scaled). Orange area delimits rod-shaped haplonemes, the blue area covers oval and round-shaped haplonemes. Smaller dots and lines represent phylogenetic relationships and ancestral states of internal nodes under BM. Species nodes in red lack either haplonemes or heteronemes, and their values projected onto the axis of the nematocyst type they bear. Cystonects have no tentacle heteronemes and are projected onto the haploneme axis. Apolemiids have no tentacle haplonemes and are projected onto the heteroneme axis.

134 siphonophore species other than Cystonects, *Apolemia*, and Pyrostephidae. There is one
 135 secondary return to more oval, less elongated haplonemes in *Erenna*, but it does not reach the
 136 sphericity present in Cystonectae or Pyrostephidae (Fig. 4). Heteroneme evolution presents a
 137 less discrete evolutionary history, where Tendiculophora evolved more elongate heteronemes,
 138 but the difference between theirs and other siphonophores is much smaller than the variation
 139 in shape within Tendiculophora, bearing no phylogenetic signal. In this clade, the evolution of
 140 heteroneme shape has diverged in both directions, and there is no correlation with haploneme
 141 shape (Fig. 4), which has remained fairly constant (elongation between 1.5 and 2.5).

142 *Phenotypic integration of the tentillum* – Of the phylogenetic correlations (SM??a, lower
 143 triangle), 81.3% were positive and 18.7% were negative, while of the ordinary correlations

¹⁴⁴ (SM??a, upper triangle) 74.6% were positive and 25.4% were negative. Half (49.9%) of
¹⁴⁵ phylogenetic correlations were >0.5 , while only 3.6% are < -0.5 . Similarly, of the across-
¹⁴⁶ species correlations, 49.1% were >0.5 and only 1.5% were < -0.5 . We found that 13.9% of
¹⁴⁷ character pairs had opposing phylogenetic and ordinary correlation coefficients. Just 4% have
¹⁴⁸ negative phylogenetic and positive ordinary correlations (such as rhopaloneme elongation \sim
¹⁴⁹ heteroneme-to-cnidoband length ratio and haploneme elongation, or haploneme elongation \sim
¹⁵⁰ heteroneme number), and only 9.9% of character pairs had positive phylogenetic correlation
¹⁵¹ yet negative ordinary correlation (such as heteroneme elongation \sim cnidoband convolution
¹⁵² and involucrum length, or rhopaloneme elongation with cnidoband length). These disparities
¹⁵³ can be caused by Simpson's paradox (16): the reversal of the sign of a relationship when a
¹⁵⁴ third variable (or a phylogenetic topology (17)) is considered. However, no character pair
¹⁵⁵ had correlation coefficient differences larger than 0.64 between ordinary and phylogenetic
¹⁵⁶ correlations (heteroneme shaft extension \sim rhopaloneme elongation has a Pearson's correlation
¹⁵⁷ of 0.10 and a phylogenetic correlation of -0.54). Rhopaloneme elongation shows the most
¹⁵⁸ incongruencies between phylogenetic and ordinary correlations with other characters.

¹⁵⁹ In the non-phylogenetic PCA morphospace using only simple characters (SM5), PC1
¹⁶⁰ (aligned with tentillum and tentacle size) explained 69.3% of the variation in the tentillum
¹⁶¹ morphospace, whereas PC2 (aligned with heteroneme length, heteroneme number, and
¹⁶² haploneme arrangement) explained 13.5%. In a phylogenetic PCA, 63% of the evolutionary
¹⁶³ variation in the morphospace is explained by PC1 (aligned with shifts in tentillum size), while
¹⁶⁴ 18% is explained by PC2 (aligned with shifts in heteroneme number and involucrum length).

¹⁶⁵ The siphonophore tentillum morphospace has a fairly low extant dimensionality due
¹⁶⁶ to having an evolutionary history with many synchronous, correlated changes. This is
¹⁶⁷ consistent with strong phenotypic integration where genetic and developmental correlations
¹⁶⁸ are maintained by natural selection to preserve a complex function across the wide variety
¹⁶⁹ of morphologies present. Since most tentillum characters develop from a common bud
¹⁷⁰ (budding tentilla near the base of the tentacle), structural correlations are expected. Similarly,

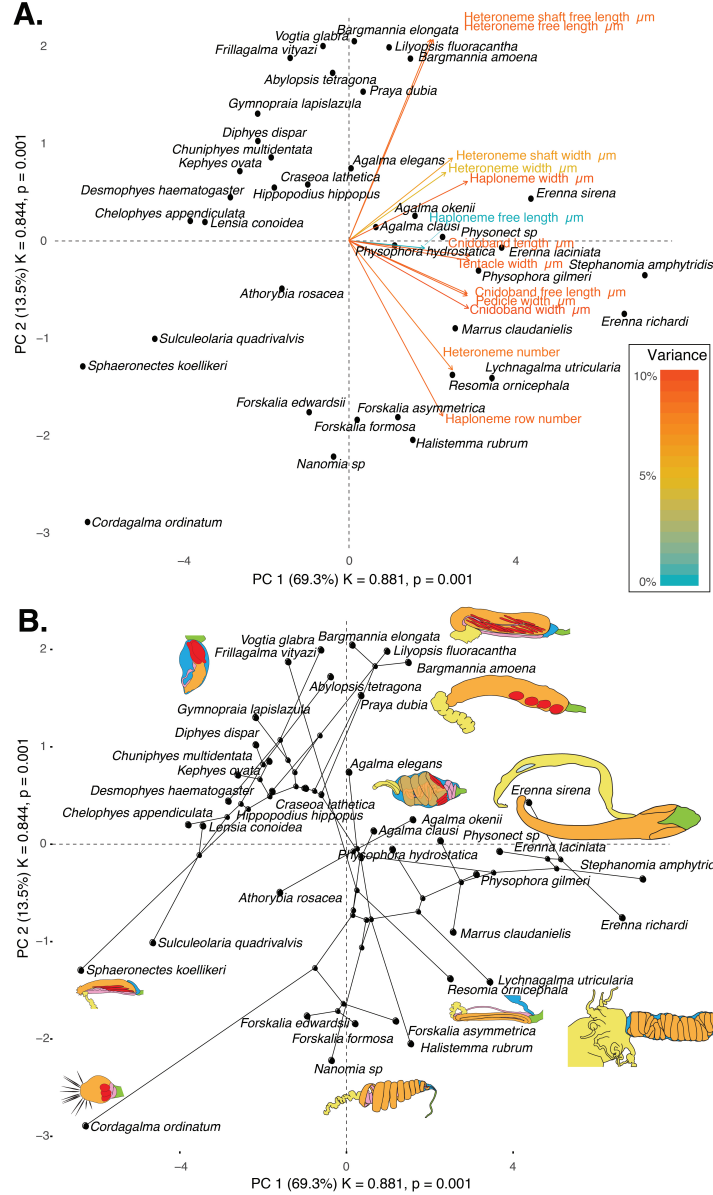


Figure 5: Phylomorphospace of the simple continuous characters principal components, excluding ratios and composite characters. A. Variance explained by each variable in the PC1-PC2 plane. Axis labels include the phylogenetic signal (K) for each component and p-value. B. Phylogenetic relationships between the species points distributed in that same space.

¹⁷¹ correlations between the features of different nematocyst subtypes within a species are also
¹⁷² expected given their common evolutionary and developmental origin (18, 19). However, we
¹⁷³ also found correlations between nematocyst and tentillum characters. Siphonophore tentacle
¹⁷⁴ nematocysts (in their cnidocytes) are not produced nor matured in the developing tentillum.
¹⁷⁵ These cnidocytes are produced by dividing cnidoblasts in the basigaster (basal swelling of
¹⁷⁶ the gastrozooid). Once the cnidocytes have assembled the nematocyst, they migrate outward
¹⁷⁷ along the tentacle (20) and position themselves in the tentillum according to their type and size
¹⁷⁸ (14). Thus, the developmental programs that produce the observed nematocyst morphologies
¹⁷⁹ are spatially separated from those producing the tentillum morphologies. Therefore, we
¹⁸⁰ hypothesize the genetic correlations and phenotypic integration between tentillum and
¹⁸¹ nematocyst characters are maintained through natural selection on separate regulatory
¹⁸² networks, out of the necessity to work together and meet the spatial, mechanical, and
¹⁸³ functional constraints of their prey capture behavior.

¹⁸⁴ *Functional morphology of tentillum and nematocyst discharge* – Tentillum and nematocyst
¹⁸⁵ discharge high speed measurements are available in the Dryad repository. While the sample
¹⁸⁶ sizes of these measurements were insufficient to draw reliable statistical results at a phyloge-
¹⁸⁷ netic level, we did observe patterns that may be relevant to their functional morphology. For
¹⁸⁸ example, cnidoband length is strongly correlated with discharge speed (p value = 0.0002).
¹⁸⁹ This is probably the sole driver of the considerable difference between euphysonect and
¹⁹⁰ calycophoran tentilla discharge speeds (average discharge speeds: 225.0mm/s and 41.8mm/s
¹⁹¹ respectively; t-test p value = 0.011), since the euphysonects have larger tentilla than the
¹⁹² calycophorans among the species recorded.

¹⁹³ We also observed that calycophoran haploneme tubules fire faster than those of eu-
¹⁹⁴ physonects (T-test p value = 0.001). Haploneme nematocysts discharge 2.8x faster than
¹⁹⁵ heteroneme nematocysts (T-test p value = 0.0012). Finally, we observed that the stenoteles
¹⁹⁶ of the Euphysonectae discharge a helical filament that “drills” itself through the medium it
¹⁹⁷ penetrates as it everts.

198 *Generating dietary hypotheses using tentillum morphology* – For many siphonophore
199 species, no feeding observations have yet been published. We generated hypotheses about
200 the diets of these understudied siphonophores based on their known tentacle morphology and
201 the associations between morphology and diet reported here for other species using the linear
202 discriminant analysis of principal components (DAPC) fitted in (1). This provides concrete
203 predictions to be tested in future work and helps extrapolate our findings to many poorly
204 known species that are extremely difficult to collect and observe. The discriminant analysis in
205 (1) for feeding guild (7 principal components, 4 discriminants) produced 100% discrimination,
206 and the highest loading contributions were found for the characters (ordered from highest
207 to lowest): Involucrum length, heteroneme volume, heteroneme number, total heteroneme
208 volume, tentacle width, heteroneme length, total nematocyst volume, and heteroneme width.
209 We used the predictions from this discriminant function to generate hypotheses about the
210 feeding guild of 45 species in the morphological dataset. This extrapolation predicts that
211 two other *Apolemia* species are gelatinous prey specialists like *Apolemia rubriversa*, and
212 predicts that *Erenna lacinata* is a fish specialist like *Erenna richardi*. When predicting
213 soft- and hard-bodied prey specialization, the DAPC achieved 90.9% discrimination success,
214 only marginally confounding hard-bodied specialists with generalists (SM??). The main
215 characters driving this discrimination are involucrum length, heteroneme number, heteroneme
216 volume, tentacle width, total nematocyst volume, total haploneme volume, elastic strand
217 width, and heteroneme length. We only selected prey types with sufficient variation in
218 the data to carry out these analyses (copepods, fish, and large crustaceans). While the
219 presence of fish or large crustaceans in the diet cannot be unambiguously discriminated using
220 tentillum morphology (SM??,SM??), specialization on fish or large crustacean prey can be
221 fully disentangled (SM??).

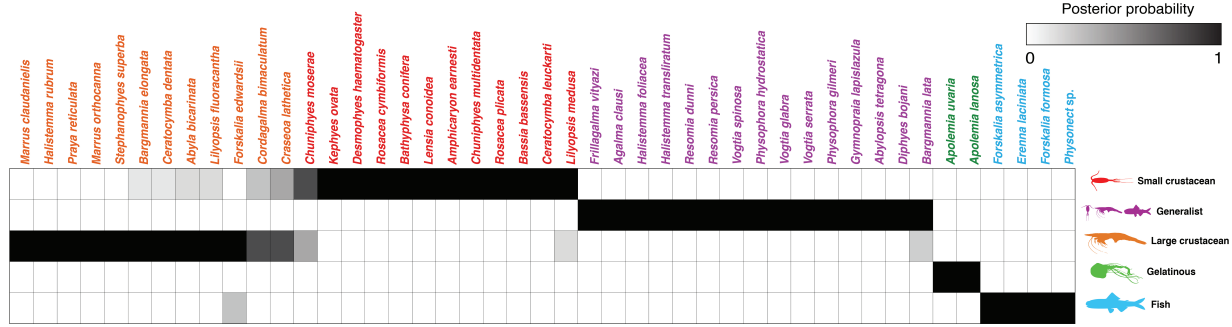


Figure 6: Hypothetical feeding guilds for siphonophore species predicted by a 6 PCA DAPC. Cell darkness indicates the posterior probability of belonging to each guild. Training data set transformed so inapplicable states are computed as zeroes. Species ordered and colored according to their predicted feeding guild.

222 Discussion

223 *On the evolution of tentilla morphology* – The evolutionary rate covariance results in (1)
 224 indicate that tentilla are not only phenotypically integrated but also show patterns of
 225 evolutionary modularity, where different sets of characters appear to evolve in stronger
 226 correlations among each other than with other characters (21). This may be indicative of the
 227 underlying genetic and developmental dependencies among closely homologous nematocyst
 228 types (such as desmonemes and rhopalonemes) and structures. In addition, these evolutionary
 229 modules point to hypothetical functional modules. For example, the coiling degree of the
 230 cnidoband and the extent of the involucrum have correlated rates of evolution, while high-
 231 speed videos (pers. obs.) show that the involucrum helps direct the whiplash of the uncoiling
 232 cnidoband distally (towards the prey). The clade Tendiculophora contains far more species
 233 than its relatives Cystonectae, Apolemiidae, and Pyrostephidae. An increase in clade richness
 234 and ecological diversification can be triggered by a ‘key innovation’ (22). The evolutionary
 235 innovation of the Tendiculophora tentilla with shooting cnidobands and modular regions may
 236 have facilitated further dietary diversification.

237 Haploneme and heteroneme shape share 21% of their variance across extant values, and
 238 53% of the variance in their shifts along the branches of the phylogeny. However, much of this
 239 correlation is due to the contrast between Pyrostephidae and their sister group Tendiculophora

240 (Fig. ??). We searched for rate regime shifts in the evolution of nematocyst shape characters
241 using a Bayesian Analysis of Macroevolutionary Mixtures (BAMM) (23) (SM32-35). BAMM
242 located a regime shift in heteroneme shape evolution on the branches leading to *Agalma* and
243 *Athorybia* (SM33). For the rates of haploneme shape evolution, BAMM identified two main
244 independent regime shifts (Fig. 4): one in the branch leading to Codonophora (anisorhizas
245 diverging from cystonects' spherical isorhizas), and one in the branch leading to Clade B
246 physonects (SM35). Clade B includes *Erenna*, *Stephanomia*, *Marrus*, and rhodaliids. Most of
247 these taxa have rod-shaped anisorhizas, but *Erenna* have oval ones. No significant regime
248 shift patterns were identified in the evolution of desmoneme and rhopaloneme shape.

249 *Heterochrony and convergence in the evolution of tentilla with diet* - In addition to
250 identifying shifts in prey type, our work reveals the specific morphological changes in the
251 prey capture apparatus associated with these changes. Copepod-specialized diets have
252 evolved convergently in *Cordagalma* and some calycophorans. These evolutionary transitions
253 happened together with transitions to smaller tentilla with fewer cnidoband nematocysts.
254 Tentilla are expensive single-use structures (24), therefore we would expect that specialization
255 in small prey would beget reductions in the size of the prey capture apparatus to the
256 minimum required for the ecological performance. *Cordagalma*'s tentilla strongly resemble
257 the larval tentilla (only found in the first-budded feeding body of the colony) of their sister
258 genus *Forskalia*. This indicates that the evolution of *Cordagalma* tentilla could be a case of
259 paedomorphic heterochrony associated with predatory specialization on smaller prey.

260 Our work identifies a novel example of convergent evolution. The region of the tentillum
261 morphospace (SM4) occupied by calycophorans was independently (and more recently)
262 occupied by the physonect *Frillagalma vityazi*. Like calycophorans, *Frillagalma* tentilla have
263 small C-shaped cnidobands with a few rows of anisorhizas. Unlike calycophorans, they lack
264 paired elongate microbasic mastigophores. Instead, they bear exactly three oval stenoteles,
265 and their cnidobands are followed by a branched vesicle, unique to this genus. Their tentillum
266 morphology is very different from that of other related physonects, which tend to have long,

267 coiled, cnidobands with many paired oval stenoteles. Most studies on calycophoran diets
268 have reported their prey to be primarily composed of small crustaceans, such as copepods
269 or ostracods (25, 26). The diet of *Frillagalma vityazi* is unknown, but this morphological
270 convergence suggests that they evolved to capture similar kinds of prey. The DAPCs in (1)
271 predict that *Frillagalma* has a generalist niche with both soft and hard-bodied prey, including
272 copepods.

273 *Evolution of nematocyst shape* – A remarkable feature of siphonophore haplonemes is
274 that they are outliers to all other Medusozoa in their surface area to volume relationships,
275 deviating significantly from sphericity (27). This suggests a different mechanism for their
276 discharge that could be more reliant on capsule tension than on osmotic potentials (28),
277 and strong selection for efficient nematocyst packing in the cnidoband (14, 27). Our results
278 show that Codonophora underwent a shift towards elongation and Cystonectae towards
279 sphericity, assuming the common ancestor had an intermediate state. Since we know that the
280 haplonemes of other hydrozoan outgroups are generally spheroid, it is more parsimonious to
281 assume that cystonects retain this ancestral state. Later, we observe a return to more rounded
282 (ancestral) haplonemes in *Erenna*, concurrent with a secondary gain of a piscivorous trophic
283 niche, like that exhibited by cystonects. (26) showed that haplonemes have a penetrating
284 function as isorhizas in cystonects and an adhesive function as anisorhizas in Tendiculophora.
285 The two clades that have converged to feed primarily on fish (Cystonectae and Clade B, which
286 includes *Erenna*, *Stephanomia*, *Marrus*, and rhodaliids) have also converged morphologically
287 toward more compact haplonemes, significantly distinct from their closest relatives. Isorhizas
288 in cystonects are known to penetrate the skin of fish during prey capture, and to deliver
289 the toxins that aid in paralysis and digestion (29). *Erenna*'s anisorhizas are also able to
290 penetrate human skin and deliver a painful sting (30) (and pers. obs.), a common feature of
291 piscivorous cnidarians like the Portuguese man-o-war or box jellies.

292 The implications of these results for the evolution of nematocyst function are that an
293 innovation in the discharge mechanism of haplonemes may have occurred during the main shift

294 to elongation. Elongate nematocysts can be tightly packed into cnidobands. We hypothesize
295 this may be a Tendiculophora lineage-specific adaptation to packing more nematocysts into a
296 limited tentillum space, as suggested by (14). (27) hypothesized that smaller, more spherical
297 nematocysts, with a lower surface area to volume ratio, are more efficient in osmotic-driven
298 discharge and thus have more power for skin penetration. The elongated haplonemes of
299 crustacean-eating Tendiculophora have never been observed penetrating their crustacean
300 prey (26), and are hypothesized to entangle the prey through adhesion of the abundant
301 spines to the exoskeletal surfaces and appendages. Entangling requires less acceleration and
302 power during discharge than penetration, as it does not rely on point pressure. In fish-eating
303 cystonects and *Erenna* species, the haplonemes are much less elongated and very effective at
304 penetration, in congruence with the osmotic discharge hypothesis. Tendiculophora, composed
305 of the clades Euphysonectae and Calycophorae, includes the majority of siphonophore species.
306 Within these clades are the most abundant siphonophore species, and a greater morphological
307 and ecological diversity is found. We hypothesize that this packing-efficient haploneme
308 morphology may have been a key innovation leading to the diversification of this clade.
309 However, other characters that shifted concurrently in the stem of this clade may have been
310 responsible for their extant diversity.

311 *Generating hypotheses on siphonophore feeding ecology* – One motivation for our research
312 was to understand the links between predator capture tools and their diets so we can generate
313 hypotheses about the diets of siphonophores based on morphological characteristics. Indeed,
314 our discriminant analyses were able to distinguish between different siphonophore diets
315 based on morphological characters alone. The models produced by these analyses generated
316 testable predictions about the diets of many species for which we only have morphological
317 data of their tentacles. While the limited dataset used here is informative for generating
318 tentative hypotheses, the empirical dietary data are still scarce and insufficient to cast robust
319 predictions. This reveals the need to extensively characterize siphonophore diets and feeding
320 habits. In future work, we can test these ecological hypotheses and validate these models

321 by directly characterizing the diets of some of those siphonophore species. Predicting diet
322 using morphology is a powerful tool to reconstruct food web topologies from community
323 composition alone. In many of the ecological models found in the literature, interactions
324 among the oceanic zooplankton have been treated as a black box (31). The ability to predict
325 such interactions, including those of siphonophores and their prey, will enhance the taxonomic
326 resolution of nutrient-flow models constructed from plankton community composition data.
327 ## Acknowledgements {-} This work was supported by the Society of Systematic Biologists
328 (Graduate Student Award to A.D.S.); the Yale Institute of Biospheric Studies (Doctoral Pilot
329 Grant to A.D.S.); and the National Science Foundation (Waterman Award to C.W.D., and
330 NSF-OCE 1829835 to C.W.D., S.H.D.H., and C. Anela Choy). A.D.S. was supported by a
331 Fulbright Spain Graduate Studies Scholarship.

332 Supplementary Materials

333 References

- 334 1. Damian-Serrano A, Haddock SH, Dunn CW (2019) The evolution of siphonophore tentilla
335 as specialized tools for prey capture. *bioRxiv*:653345.
- 336 2. Harmon LJ, Weir JT, Brock CD, Glor RE, Challenger W (2007) GEIGER: Investigating
337 evolutionary radiations. *Bioinformatics* 24(1):129–131.
- 338 3. Sugiura N (1978) Further analysts of the data by akaike's information criterion
339 and the finite corrections: Further analysts of the data by akaike's. *Communications in
340 Statistics-Theory and Methods* 7(1):13–26.
- 341 4. Pennell MW, FitzJohn RG, Cornwell WK, Harmon LJ (2015) Model adequacy and the
342 macroevolution of angiosperm functional traits. *The American Naturalist* 186(2):E33–E50.
- 343 5. Blomberg SP, Garland T, Ives AR (2003) Testing for phylogenetic signal in comparative
344 data: Behavioral traits are more labile. *Evolution* 57(4):717–745.
- 345 6. Revell LJ (2012) Phytools: An r package for phylogenetic comparative biology (and

Character	Non-Phylogenetic dAIC	BM dAIC	EB dAIC	OU dAIC	K	K p-value	Ntaxa
Haploneme elongation	0	2.017	4.332	2.38	0.583	0.001	43
Desmoneme elongation	0	3.232	5.693	3.183	0.018	0.864	31
Heteroneme shaft width μm	0	5.346	7.67	2.581	0.45	0.005	42
Elastic strand width μm	0	1526	3.938	1.296	0.706	0.001	34
Desmoneme length μm	0.518	0	2.46	0.578	0.566	0.002	31
Heteroneme shaft extension	0.589	0	2.324	1.965	0.041	0.970	42
Haploneme SA/V	0.91	0	2.315	2.291	0.156	0.132	43
Total heteroneme volume μm^3	0.961	0	2.352	2.328	0.248	0.046	39
Rhopaloneme width μm	1.205	0	2.46	1.321	0.308	0.123	31
Heteroneme volume μm^3	2.002	0	2.153	2.324	0.196	0.117	42
Involucrum length μm	2.479	0	2.498	2.492	0.529	0.001	29
Tentacle width μm	2.939	0	2.307	1.974	0.367	0.044	44
Cnidoband coiledness	3.077	0	2.315	1.786	0.174	0.043	43
Total haploneme volume μm^3	3.641	0	1.852	2.296	0.198	0.267	43
Cnidoband free length μm	3.801	0	2.132	2.315	0.325	0.007	43
Heteroneme free length μm	3.82	0	2.01	1.325	0.301	0.080	42
Rhopaloneme elongation	3.852	0	2.145	2.46	0.062	0.827	31
Desmoneme width μm	3.96	0	2.46	2.121	0.553	0.004	31
Cnidoband length μm	4.094	0	1.911	2.315	0.321	0.015	43
Heteroneme number	4.262	0	2.352	2.219	0.866	0.001	39
Heteroneme shaft free length μm	4.553	0	2.324	2.321	0.331	0.126	42
Rhopaloneme length μm	5.599	0	2.46	2.457	0.589	0.001	31
Heteroneme/Cnidoband length	5.671	0	1.862	2.342	1.068	0.001	42
Pedicle width μm	6.566	0	2.253	2.315	0.541	0.001	43
Haploneme width μm	7.495	0	2.218	2.304	0.553	0.001	43
Heteroneme width μm	7.53	0	2.324	1.647	0.502	0.001	42
Heteroneme elongation	14.169	0	0.819	2.23	0.508	0.001	42
Haploneme row number	19.566	0	2.114	2.315	0.442	0.001	43
Total nematocyst volume μm^3	21.007	0	2.213	2.292	1.3	0.001	45
Cnidoband width μm	5.69	0.307	0	2.623	0.374	0.001	43
Haploneme free length μm	12.337	7.125	0	9.439	1.079	0.001	43

Non-phylogenetic model supported

Brownian Motion model supported

Early Burst model supported

Figure 7: Model support (delta AICc), phylogenetic signal (Blomberg's K), and phylogenetic signal permutation test p-value for each continuous character. Ntaxa = Number of taxa used in the analyses after removing those where the character state is inapplicable or the data is missing.

Variable	Best model	Msig	Cvar	Svar	Sasr	Shgt	Dcfid
Desmoneme length μm	WN	0.889	0.224	0.084	0.32	0.146	0
Heteroneme shaft extension	WN	0.861	0	0.577	0	0.533	0.042
Total heteroneme volume	WN	0.895	0.577	0.006	0.026	0.078	0.603
Rhopaloneme width μm	WN	0.823	0.42	0.182	0.014	0.531	0.006
Haploneme free length μm	EB	0.841	0.052	0.036	0.168	0.226	0.843
Heteroneme volume μm^3	BM	0.855	0.731	0.228	0.897	0.775	0.104
Involucrum length μm	BM	0.839	0.01	0.018	0.116	0.09	0.987
Tentacle width μm	BM	0.817	0.841	0.402	0.386	0.785	0.48
Cnidoband coiledness	BM	0.873	0	0.028	0.016	0.144	0.41
Total haploneme volume	BM	0.807	0.228	0.004	0.006	0.024	0.398
Cnidoband free length μm	BM	0.825	0.076	0.002	0	0.006	0.681
Heteroneme free length μm	BM	0.859	0.392	0.386	0.056	0.591	0.284
Rhopaloneme elongation	BM	0.873	0.022	0.006	0.004	0.048	0.104
Desmoneme width μm	BM	0.813	0.877	0.531	0.014	0.941	0.014
Cnidoband length μm	BM	0.829	0.096	0	0	0.004	0.901
Heteroneme number	BM	0.823	0.312	0	0.004	0.02	0.869
Heteroneme shaft free length μm	BM	0.877	0.468	0.565	0.034	0.841	0.851
Rhopaloneme length μm	BM	0.829	0.525	0.547	0.01	0.917	0.08
Heteroneme/cnidoband length	BM	0.839	0.01	0	0.004	0.008	0.715
Cnidoband width μm	BM	0.907	0.977	0	0.002	0.01	0.11
Pedicle width μm	BM	0.817	0.931	0.476	0.088	0.969	0.813
Haploneme width μm	BM	0.881	0.805	0.12	0.294	0.511	0.15
Heteroneme width μm	BM	0.849	0.142	0.156	0.356	0.819	0.278
Heteroneme elongation	BM	0.933	0.094	0.07	0.681	0.791	0.777
Haploneme row number	BM	0.863	0	0.002	0.004	0.008	0.012

Figure 8: Model adequacy scores for the best model supported for each morphological character. Cvar = coefficient of variation of the absolute value of the contrasts. Svar = Slope of a linear model fitted to the absolute value of the contrasts against their expected variances. Sasr = slope of the contrasts against the ancestral state inferred at each corresponding node. Shgt = slope of the contrasts against node depth. Dcfid = Kolmogorov-Smirnov D-statistic comparing contrasts to a normal distribution with SD equal to the root of the mean of squared contrasts.

- ³⁴⁶ other things). *Methods in Ecology and Evolution* 3(2):217–223.
- ³⁴⁷ 7. Felsenstein J (1985) Phylogenies and the comparative method. *The American Naturalist*
- ³⁴⁸ 125(1):1–15.
- ³⁴⁹ 8. Revell LJ, Chamberlain SA (2014) Rphylip: An r interface for phylip. *Methods in*
- ³⁵⁰ *Ecology and Evolution* 5(9):976–981.
- ³⁵¹ 9. Pugh P, Baxter E (2014) A review of the physonect siphonophore genera halistemma
- ³⁵² (family agalmatidae) and stephanomia (family stephanomiidae). *Zootaxa* 3897(1):1–111.
- ³⁵³ 10. Totton AK, Bargmann HE (1965) *A synopsis of the siphonophora* (British Museum
- ³⁵⁴ (Natural History)).
- ³⁵⁵ 11. Bardi J, Marques AC (2007) Taxonomic redescription of the portuguese man-of-war,
- ³⁵⁶ physalia physalis (cnidaria, hydrozoa, siphonophorae, cystonectae) from brazil. *Iheringia*
- ³⁵⁷ *Série Zoologia* 97(4):425–433.
- ³⁵⁸ 12. Munro C, et al. (2018) Improved phylogenetic resolution within siphonophora
- ³⁵⁹ (cnidaria) with implications for trait evolution. *Molecular Phylogenetics and Evolution*.
- ³⁶⁰ 13. Siebert S, Pugh PR, Haddock SH, Dunn CW (2013) Re-evaluation of characters in
- ³⁶¹ apolemiidae (siphonophora), with description of two new species from monterey bay, california.
- ³⁶² *Zootaxa* 3702(3):201–232.
- ³⁶³ 14. Skaer R (1988) *The formation of cnidocyte patterns in siphonophores* (Academic
- ³⁶⁴ Press New York).
- ³⁶⁵ 15. Skaer R (1991) Remodelling during the development of nematocysts in a siphonophore.
- ³⁶⁶ *Hydrobiologia* (Springer), pp 685–689.
- ³⁶⁷ 16. Blyth CR (1972) On simpson's paradox and the sure-thing principle. *Journal of the*
- ³⁶⁸ *American Statistical Association* 67(338):364–366.
- ³⁶⁹ 17. Uyeda JC, Zenil-Ferguson R, Pennell MW (2018) Rethinking phylogenetic comparative
- ³⁷⁰ methods. *Systematic Biology* 67(6):1091–1109.
- ³⁷¹ 18. Bode H (1988) Control of nematocyte differentiation in hydra. *The Biology of*
- ³⁷² *Nematocysts* (Elsevier), pp 209–232.

- 373 19. David CN, et al. (2008) Evolution of complex structures: Minicollagens shape the
374 cnidarian nematocyst. *Trends in genetics* 24(9):431–438.
- 375 20. Carré D (1972) Study on development of cnidocysts in gastrozooids of muggiaeae kochi
376 (will, 1844) (siphonophora, calycophora). *Comptes Rendus Hebdomadaires des Seances de*
377 *l'Academie des Sciences Serie D* 275(12):1263.
- 378 21. Wagner GP (1996) Homologues, natural kinds and the evolution of modularity.
379 *American Zoologist* 36(1):36–43.
- 380 22. Simpson GG (1955) *Major features of evolution* (Columbia University Press: New
381 York).
- 382 23. Rabosky DL, et al. (2014) BAMM tools: An r package for the analysis of evolutionary
383 dynamics on phylogenetic trees. *Methods in Ecology and Evolution* 5(7):701–707.
- 384 24. Mackie GO, Pugh PR, Purcell JE (1987) Siphonophore Biology. *Advances in Marine
385 Biology* 24:97–262.
- 386 25. Purcell J (1981) Dietary composition and diel feeding patterns of epipelagic
387 siphonophores. *Marine Biology* 65(1):83–90.
- 388 26. Purcell JE (1984) The functions of nematocysts in prey capture by epipelagic
389 siphonophores (coelenterata, hydrozoa). *The Biological Bulletin* 166(2):310–327.
- 390 27. Thomason J (1988) The allometry of nematocysts. *The Biology of Nematocysts*
391 (Elsevier), pp 575–588.
- 392 28. Carré D, Carré C (1980) On triggering and control of cnidocyst discharge. *Marine &
393 Freshwater Behaviour & Phy* 7(1):109–117.
- 394 29. Hessinger DA (1988) Nematocyst venoms and toxins. *The Biology of Nematocysts*
395 (Elsevier), pp 333–368.
- 396 30. Pugh P (2001) A review of the genus erenna bedot, 1904 (siphonophora, physonectae).
397 *BULLETIN-NATURAL HISTORY MUSEUM ZOOLOGY SERIES* 67(2):169–182.
- 398 31. Mitra A (2009) Are closure terms appropriate or necessary descriptors of zooplankton
399 loss in nutrient–phytoplankton–zooplankton type models? *Ecological Modelling* 220(5):611–

₄₀₀ 620.